

Automatic Salient Object Detection for Panoramic Images Using Region Growing and Fixation Prediction Model

Chunbiao Zhu*, Kan Huang, Ge Li

School of Electronic and Computer Engineering,
Shenzhen Graduate School,
Peking University
Shenzhen, China

*zhuchunbiao@pku.edu.cn

Abstract

Most previous works on saliency detection are dedicated to conventional images, however, it is becoming more and more vital to obtain visual attention for panoramic images with the rapid development of VR or AR technology. In this paper, we propose a novel automatic salient object detection framework for panoramic images using region growing and fixation prediction model. First, we employ a spatial density pattern detection method using region growing for the panoramic image to roughly extract the proposal objects. Meanwhile, the eye fixation model is embedded into the framework to predict the visual attention, which simulates the human vision system. Then, the previous saliency information is combined by the maxima normalization to get the coarse saliency map. Finally, a geodesic refinement is utilized to obtain the final saliency map. To fairly evaluate the performance of the proposed framework, we build a new high-quality dataset of panoramic images for the public. Extensive evaluations performed on the new dataset (SalPan) show the superiority of the proposed framework than other methods.

Introduction

An inherent and powerful ability of human eyes is to quickly capture the most conspicuous regions from a scene, and passes them to high-level visual cortexes. The attention selection reduces the complexity of visual analysis and thus makes human visual system considerably efficient in complex scenes. As a pre-processing procedure, many applications benefit from saliency analysis, such as detecting abnormal pattern (Itti, Koch, and Niebur 1998), segmenting proto-objects (Hou and Zhang 2007), generating object proposals (Alexe, Deselaers, and Ferrari 2012) etc. The concept of saliency are investigated not only in early vision modeling but also in many engineering applications such as image compression (Itti 2004), object recognition (Salah, Alpaydin, and Akarun 2002) and tracking (Frintrop 2010), robot navigation (Siagian and Itti 2009), advertising (Rosenholtz, Dorai, and Freeman 2011) etc.

Early work on computing saliency aimed to model and predict human gaze on images (Itti, Koch, and Niebur 1998). Recently the field has expanded to include the segmentation of entire salient regions or objects (Achanta and Hemami 2009).

Most works extract salient regions which exhibit highly distinct features compared to their surrounding regions, based on the concept of center-surround contrast. Moreover, additional prior knowledge for spatial layout of foreground objects and background can be also used: have a high possibility for belonging to the background (Wei and Wen 2012; Zhu and Liang 2014), while foreground salient objects are often located near the image center (Cheng and Warrell 2013; Margolin and Tal 2013). These assumptions have been successfully employed to improve the performance of saliency detection for conventional images with common aspect ratios.

Recently, panoramic images, which yield wide fields of view, become popular in all kinds of media contents and draw much attention in many practical applications. For example, virtual reality contents exhibit wide fields of view when used for wearable devices such as the head-mounted display. Around-view monitoring systems for autonomous vehicles use panoramic images by combining multiple images captured at different viewing positions. These panoramic images can be directly obtained by using special devices, or can be generated by combining several conventional images with small aspect ratios using image stitching techniques (Lin and Pankanti 2015). However, the assumptions used for detecting saliency of conventional images do not completely reflect the characteristics of panoramic images. Therefore, it takes more interest to develop efficient processing techniques for panoramic images.

In this work, we propose an automatic salient object detection framework for panoramic images using region growing and fixation prediction model. Panoramic images exert several distinct characteristics compared to conventional images. A panoramic image has a much larger width than height, and hence the background is distributed over horizontally elongated area. Moreover, the background is usually composed of several homogeneous regions such as sky, mountain, and ground. Also, a typical panoramic image may include multiple foreground objects with different features and sizes, which are arbitrarily located in an image. Due to these characteristics, it is difficult to design a global approach to extract multiple salient regions directly from an input panoramic image. We find that spatial density patterns is useful in images with high resolutions. Therefore, we first employ a spatial density pattern detection method based on

region growing for the panoramic image to roughly extract the proposal objects. And the eye fixation model is embedded into the framework to predict the visual attention, which is inspired by the human vision system. Then, the previous saliency information is combined by the maxima normalization to derive the coarse saliency map. Finally, a geodesic refinement is employed to obtain the final saliency map.

The main contributions of this paper are listed as follows:

1. A new automatic salient object detection framework is proposed for panoramic images combining region growing and eye fixation model.
2. The spatial density pattern detection algorithm using region growing is first introduced in the field of saliency detection.
3. To fairly evaluate the performance of the proposed method, we build a new high-quality panoramic dataset (SalPan) with a novel ground truth annotation method which can eliminate the ambiguous of salient objects. This SalPan dataset will be public shortly.
4. The proposed framework is also fit for small target detection and conventional images' saliency detection.

We also think that this research may help to figure out the perception characteristics of the human visual system for large-scale visual contents over a wide field of view.

The rest of this paper is organized as follows. Section 2 briefly reviews related work. Section 3 explains the proposed framework. Section 4 presents the experimental results. Section 5 discusses some practical guidelines. Section 6 concludes this paper.

Related Works

In this section, we have a brief review of classical eye fixation models and traditional saliency algorithms.

Eye Fixation Model

The first models for saliency prediction were biologically inspired and based on a bottom-up computational model that extracted low-level visual features such as intensity, color, orientation, texture and motion at multiple scales. Itti et al. (Itti, Koch, and Niebur 1998) proposed a model that combines multiscale low-level features to create a saliency map. Harel et al. (Harel and Koch 2007) presented a graph-based alternative that starts from low-level feature maps and creates Markov chains over various image maps, treating the equilibrium distribution over map locations as activation and saliency values.

These models achieved a reasonable result, however, the models had limited use because they frequently did not match actual human saccades from eye-tracking data. It seemed that humans not only base their attention on low-level features, but also on high-level semantics (Cerf and Harel 2008) (e.g., faces, humans, cars, etc.). Judd et al. (Judd 2009) introduced an approach that combined low, mid and high-level image features to calculate salient locations. These features were used in combination with a linear support vector machine to train a saliency model. Borji (Borji 2012) also combined low-level features with

top-down cognitive visual features and learned a direct mapping to eye fixations using Regression, SVM and AdaBoost classifiers. Since the eye fixation model can mimic the process of the human visual system, thus, we embed the fixation prediction model into our framework.

Traditional Saliency Algorithm

Saliency detection for conventional images could be implemented based on either top-down or bottom-up models. Top-down models (Oliva and Torralba 2003; Gao and Vasconcelos 2005; Gao and Han 2009; Yang 2012) required high level interpretation usually provided by training sets in supervised learning. Contextual saliency was formulated according to the study of visual cognition: global scene context of an image was highly associated with a salient object (Oliva and Torralba 2003). The most distinct features were selected by information theory based methods (Gao and Vasconcelos 2005; Gao and Han 2009). Salient objects were detected by joint learning of a dictionary for object features and conditional random field classifiers for object categorization (Yang 2012). While these supervised approaches can effectively detect salient regions and perform overall better than bottom-up approaches, it is still expensive to perform the training process, especially data collection.

In contrary, bottom-up models (Qin and Lu 2015; Li and Lu 2015; Shi and Yan 2016; Zhu and Li 2017) did not require prior knowledge such as object categories, but obtained saliency maps by using low level features based on the center-surround contrast. They computed feature distinctness of a target region, e.g., pixel, patch or superpixel, compared to its surrounding regions locally or globally. For example, feature difference was computed across multiple scales, where a fine scale feature map represented the feature of each pixel while a coarse scale feature map described the features of surrounding regions (Itti, Koch, and Niebur 1998). Also, to compute center-surround feature contrast, spatially neighboring pixels were assigned different weights (Perazzi 2012), or random walk on a graph was used (Kim 2014).

In addition, most bottom-up models were based on center prior or boundary prior. The center prior assumed that foreground salient objects were usually positioned near the image center, and thus assigned high saliency values (Cheng and Warrell 2013; Luo and Yuan 2011; Margolin and Tal 2013; Yang and Zhang 2013). A distance of pixels from the image center was combined with other features to reduce the contribution of pixels far from the image center to compute object saliency (Cheng and Warrell 2013). To emphasize the region near the image center, an initial saliency map was multiplied by a Gaussian distribution centered in the image (Luo and Yuan 2011). Multiple Gaussian distribution maps were also employed to weight the features of pixels adaptively according to the locations of salient objects in an image (Margolin and Tal 2013). Convex-hull was used to estimate the center of a salient object when it was not strictly positioned at the image center (Yang and Zhang 2013). However, this assumption put a strict constraint on the location of foreground object in an image, and thus might not be applicable to various images. Bottom-up based ap-

proaches did not need data collection and training process, consequently requiring little prior knowledge. These advantages make bottom-up approaches more efficient and easy to implement in a wide range of real computer vision applications. In this paper, we focus on the bottom-up approach.

The Proposed Framework

Here we describe the proposed framework in four main steps. First, we employ a region-growing algorithm for salient regions proposal. Second, an eye fixation prediction model is used to calculate a saliency map, which is then combined with salient regions proposed in the previous step to form a stable saliency map. Third, a maxima normalization is utilized to combine the previous saliency information. Fourth, the final saliency map is obtained by a refinement method that is based on geodesic distance. The main framework is depicted in Fig. 1.

Region-growing Based Detection

In this section, we aim to roughly extract regions that have significant and different densities compared with its neighbors. To our consideration, significant-different regions can be divided into three categories: 1) Over-Density, 2) Under-Density, 3) regions surrounded by Ridges or Ditches. The third one may capture regions surrounded with a very thin edge, either a ridge or ditch, which may be easily missed out. Significant-different region detection has a great potential for salient region proposal, since salient regions always possess distinctive features compared with its surroundings.

At the beginning, the original image is partitioned into $M \times N$ grid and transformed into a density matrix, where each entry (i, j) represents the count of objects inside (i, j) th cell. Based on this density matrix, which is processed as an intensity image, image processing techniques such as image morphological operators and enhancement techniques are applied and then a region growing based algorithm is applied to extract the significant-different regions. Compared with other techniques, which only output a rough rectangular bounding box, this algorithm can return the exact shape of the significant-different regions.

For the simplicity, we transform the original color image to gray scale image, and then apply an object proposal algorithm to the gray-scale image. Thus the resulted image can be seen as the density map.

Some issues involved in region growing are considered as follows: (a) Improve the density image. We apply morphological operations, including morphological dilation, erosion, open and close to remove noises like very small regions, and connect separate homogeneous regions that are near to each other. (b) Rule out distinct background regions. Some hints are used in a post-processing step such as average intensity values and the total area of the extracted region to exclude undesirable results. (c) Seed selection. In the implementation, both automatic seed selection and iterative thresholding is provided. The automatic selection appears to achieve a favorable performance, thus it is adopted as seed selection method in the proposed approach. (d) Thresholding. Otsu's method is used for adaptive thresholding.

The experimental results show that the proposed region growing based algorithm works well in detecting significant-different regions with efficient computational power. After density estimation, we get some proposed salient regions which can be enhanced and re-examined in the next section.

Fixation prediction

Whether a location is salient or not largely depends on how much it attracts human attention. A large number of recent works on eye fixation prediction have revealed more or less the nature of this issue. Eye fixation prediction models simulate the mechanisms of the human visual system, and thus can predict the probability of a location to attract human attention. So in this section, we use eye fixation model to help us ensure which region has more power to grab human attention.

Panoramic images are often with wide fields of view, and consequently are computationally more expensive compared with conventional images. Algorithms based on color contrast, local information are not suitable for being a preprocessing step for panoramic images, for these algorithms are time-consuming and would spend a lot of computational resources. Thus we are seeking a more efficient method to help us to rapidly scan the image and roughly locate where attract human attention. Obviously Fixation prediction models in frequency domain fit this demand, for these models are computationally efficient and easy to implement.

The signature model approximately isolate the spatial support of foreground by taking the sign of the mixture signal x in the transformed domain and then transform it back to spatial domain, i.e., by computing the reconstructed image $\bar{x} = IDCT[sign(\hat{x})]$. \hat{x} stands for DCT transform of x . The image signature is defined as

$$IS(x) = sign(DCT(x)). \quad (1)$$

And the saliency map is formed by smoothing the squared reconstructed image defined above

$$S_m = g * (\bar{x} \circ \bar{x}), \quad (2)$$

where g is a Gaussian kernel.

The image signature is a simple yet powerful descriptor of natural scenes, and it can be used to approximate the spatial location of a sparse foreground hidden in a spectrally sparse background. Compared with other eye fixation models, image signature has a more efficient implementation, which runs faster than all other competitors.

To combine the proposed salient regions in previous section with saliency map S_m produced by image signature, we assign the saliency value of the proposed salient regions by averaging the saliency values of all its pixels inside. For convenience we denote the resulted saliency map as S_p . That is, for a proposed region p , its saliency value is defined as

$$S_p(i) = (\sum_{i \in p} S_m(i)) / A(p), \quad i \in p, \quad (3)$$

where $A(p)$ denote the number of pixels in the p th region.

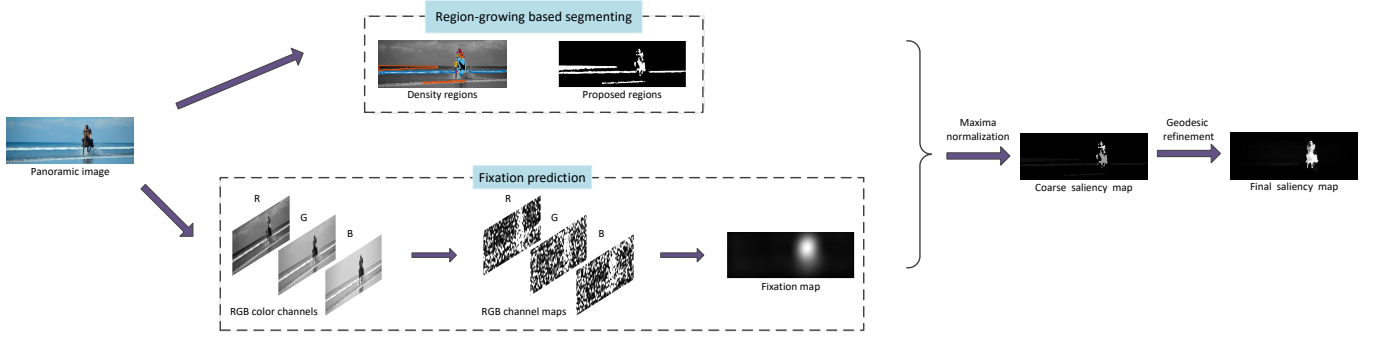


Figure 1: The framework of the proposed algorithm. **Top:** Region-growing based segmentation. **Bottom:** Fixation prediction algorithm. The temporal outputs of the two pathways are integrated using maxima normalization.

Maxima Normalization

Fusing saliency detection results of multiple models has been recognized as a challenging task since the candidate models are usually developed based on different cues or assumptions. Fortunately, in our case, the integration problem is relatively easier since we only consider the outputs from two pathways. Since there is no prior knowledge or other top-down guidance can be used, it is safer to utilize the map statistics to determine the importance of each pathway. Intuitively in the final integration stage, we combine the results from two pathways by summing them after Maxima Normalization (MN) (Algorithm 1).

Algorithm 1 Maxima Normalization $N_{max}(S, t)$

Input: Previous maps S , thresh of local maxima $t = 0.1$;

Output: Normalized Saliency Map S_N ;

```

1: Set the number of maxima  $N_M = 0$  ;
2: Set the sum of the maxima  $V_M = 0$  ;
3: Set Global Maxima  $G_M = \max(S)$  ;
4: for all pixel  $(x, y)$  of  $S$  do :
5:   if  $S(x, y) > t$  then
6:      $R = S(i, j) | i = x - 1, x + 1, j = y - 1, y + 1$  .
7:     if  $S(x, y) > \max(R)$  then
8:        $V_M = V_M + S(x, y)$  .
9:        $N_M = N_M + 1$  .
10:    end for
11:  end for
12: end for
13:  $S_N = S \cdot (G_M - V_M/N_M)^2 / G_M$  .
14: return return Normalized map  $S_N$ 

```

The Maxima Normalization operator $N_{max}(\cdot)$ was originally proposed for the integration of conspicuous maps from multiple feature channels (Itti, Koch, and Niebur 1998), which has been demonstrated very effective and has a very convincing psychological explanation.

Geodesic refinement

The final step of our proposed approach is refinement with geodesic distance (Tenenbaum J B, De Silva V, and Langford 2000). The motivation underlying this operation is

based on thought that determining saliency of an element as weighted sum of saliency of its surrounding elements, where weights are corresponding to Euclidean distance, has a limited performance in uniformly highlighting salient object. We tend to find a solution that could enhance regions of salient object more uniformly. From recent works (Zhu and Liang 2014; Fu and Gong 2013), we found the weights may be sensitive to geodesic distance.

The input image is first segmented into a number of superpixels based on linear spectral clustering method (Perazzi 2012) and the posterior probability of each superpixel is calculated by averaging the posterior probability values S_p of all its pixels inside. For j th superpixel, if its posterior probability is labeled as $\bar{S}(j)$, thus the saliency value of the q th superpixel is refined by geodesic distance as follows:

$$S(q) = \sum_{j=1}^J w_{qj} \cdot \bar{S}(j), \quad (4)$$

where J is the total number of superpixels, and w_{qj} will be a weight based on geodesic distance (Zhu and Liang 2014) between q th superpixel and j th superpixel.

The weight values are produced similar to the work (Fu and Gong 2013). First, an undirected weight graph has been constructed connecting all adjacent superpixels (a_k, a_{k+1}) and assigning their weight $d_c(a_k, a_{k+1})$ as the Euclidean distance between their saliency values which are derived in the previous section. Then the geodesic distance between two superpixels $d_g(p, i)$ can be defined as accumulated edge weights along their shortest path on the graph:

$$d_g(p, i) = \min_{a_1=p, a_2, a_3, \dots, a_n=i} \sum_{k=1}^{n-1} d_c(a_k, a_{k+1}). \quad (5)$$

In this way we can get geodesic distance between any two superpixels in the image. Then the weight δ_{pi} is defined as

$$\delta_{pi} = \exp\left\{-\frac{d_g^2(p, i)}{2\sigma_c^2}\right\}, \quad (6)$$

where σ_c is the deviation for all d_c values. From formula (6) we can easily conclude that when p and i are in flat region, saliency value of i would have a higher contribution

to saliency value of p , and when p and i are in different regions between which a steep slope is existed, saliency value of i tends to have a less contribution to saliency value of p . The effectiveness of geodesic refinement is also illustrated in Fig.1 The salient objects are highlighted uniformly after this step of processing.

Experiments

To fairly evaluate the performance of the proposed framework, we build a new dataset of panoramic landscape images (SalPan), and evaluate the performance of the proposed saliency detection algorithm compared with six state-of-the-arts methods. More experimental analysis on the effectiveness of our method are given as follows.

Datasets

We collect a new panoramic dataset SalPan composed of 115 panoramic images: 20 images are taken by ourselves, and 95 images are collected from websites. In general, saliency may be ambiguous in images with highly complex scenes and wide fields of view, thus we propose a novel ground truth annotation method (Fig. 2) to eliminate the ambiguous. We first use eye fixation equipment to tracking eye movement. Then, we record the tracking path and allocate values to each eye movement location according to the times of visual attention. Finally, we pick up those values above the average and label the ground truth with complete objects corresponding attention points. The process of labeling the ground truth is shown in Fig. 2.

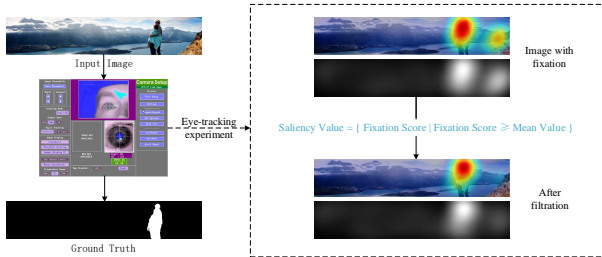


Figure 2: The process of generating the ground truth for the SalPan dataset.

Meanwhile, we make the image acquisition and image annotation independent to each other, we can avoid dataset design bias, namely a specific type of bias that is caused by experimenters' unnatural selection of dataset images. After picking up the salient regions, we adhere to the following rules to build the ground truth:

- 1) disconnected regions of the same objects are labeled separately;
- 2) solid regions are used to approximate hollow objects, such as bike wheels.

Besides, we will expand this dataset further in future.

Evaluation indicators

Experimental evaluations are based on standard measurements including precision-recall curve, precision value, re-

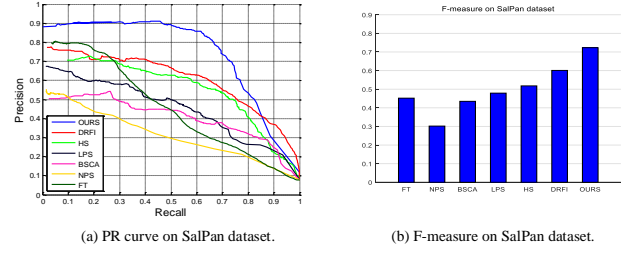


Figure 3: Visual comparisons of different saliency algorithms on SalPan dataset.

call value, AUC value, MAE (Mean Absolute Error) value, time-consuming with coding type and F-measure. The precision is defined as:

$$Precision = \frac{\|p_i \mid d(p_i) \geq d_t \cap p_g\|}{\|p_i \mid d(p_i) \geq d_t\|}, \quad (7)$$

where $p_i \mid d(p_i) \geq d_t$ indicates the set that binarized from a saliency map using threshold d_t . p_g is the set of pixels belonging to groundtruth salient object.

The recall is defined as:

$$Recall = \frac{\|p_i \mid d(p_i) \geq d_t \cap p_g\|}{\|p_g\|}. \quad (8)$$

The precision-recall curve is plotted by connecting the P-R scores for all thresholds.

The MAE is formulated as:

$$MAE = \frac{\sum_{i=1}^N \|GT_i - S_i\|}{N}, \quad (9)$$

where N is the number of the testing images, GT_i is the area of the ground truth of an image i , S_i is the area of the result of an image i .

The F-measure is formulated as:

$$F - measure = \frac{(1 + \beta^2) \times Precision \times Recall}{\beta^2 \times Precision + Recall}, \quad (10)$$

where β^2 is set to 0.3 as did in many literatures.

Comparison

To illustrate the effectiveness of our algorithm, we compare our proposed methods with FT (Achanta and Hemami 2009), NPS (Hou and Zhang 2009), BSCA (Qin and Lu 2015), LPS (Li and Lu 2015), HS (Shi and Yan 2016) and DRFI (Wang and Jiang 2017). We use the codes provided by the authors to reproduce their experiments. For all the compared methods, we use the default settings suggested by the authors.

Fig. 3(a) compares the PR curves, where we see that the proposed algorithm achieves a much higher performance than that of the existing methods.

As observed in Fig. 3(b), we see that the proposed algorithm has a higher F-measure score than any other competitors.

Method	FT	NPS	BSCA	LPS	HS	DRFI	OURS
MAE	0.3868	0.3613	0.4137	0.3697	0.4090	0.3592	0.2744
AUC	0.507	0.421	0.511	0.518	0.681	0.701	0.802
Precision	0.463	0.403	0.471	0.486	0.559	0.631	0.714
Recall	0.428	0.419	0.406	0.479	0.569	0.627	0.675
Time(s)	0.593	2.397	1.276	2.193	2.896	1.903	1.875
Code	C++	MATLAB	MATLAB	MATLAB & C++	MATLAB & C++	MATLAB & C++	MATLAB

Table 1: Evaluation indicators on SalPan dataset.



Figure 4: Visual comparisons of different saliency algorithms on SalPan dataset. From top to bottom: input panoramic images, the resulting saliency maps obtained by FT, NPS, BSCA, LPS, HS, DRFI, and the saliency maps of the proposed algorithm, respectively. The last row shows the ground truth (GT).

We measure the MAE value, precision value, recall value and AUC value using a resulting saliency map against the ground truth saliency map, which are shown in Table 1. We have seen that the proposed algorithm also achieves the best performance and outperforms all other compared methods.

We also compare the average execution times of the proposed algorithm and the other methods in Table 1. Most of the methods including the proposed one are implemented using MATLAB and executed on an Intel i7 3.4 GHz CPU with 16 GB RAM. Results show that most of the existing

methods consume more time than the proposed algorithm.

In summary, from the comparison, we can conclude that our saliency results are more robustness and efficient on SalPan dataset. Besides, the visual comparisons shown in Fig. 4 clearly demonstrate the advantages of the proposed method. We can see that our method can extract both single and multiple salient objects precisely. In contrast, the compared methods may fail in some situations.

Discussion

It is very interesting to find that the proposed automatic salient object detection algorithm for panoramic images using region growing and eye fixation model is also valid for small target detection and conventional images. We present a part of our experimental results on the small target dataset (Lou and Wang 2016) and conventional images dataset (Shi and Yan 2016). Small target detection plays an important role in many computer vision tasks, including early alarming system, remote sensing and visual tracking. The experimental results by applying the proposed algorithm to small target detections and salient detection for conventional images are shown in Fig. 5 and Fig. 6, respectively, which support our claim.

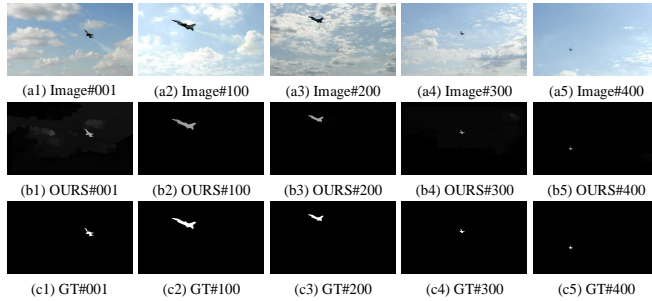


Figure 5: The proposed algorithm is applied in small target detection. (a1)-(a5) represent different frames of original video. (b1)-(b5) represent different frames of the proposed algorithm detection results. (c1)-(c5) represent different frames of the ground truth.

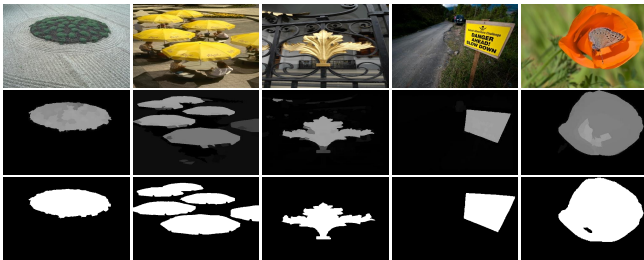


Figure 6: The proposed algorithm is used for conventional images. From top to bottom, we show input conventional images, the resulting saliency maps obtained by the proposed algorithm and ground truth.

The underlying reason why the proposed algorithm can be applied in small target detection and conventional images' saliency detection is that: the panoramic images also contain small objects and big objects, so, the image with the small target and conventional image can be seen as the part of its.

Therefore, we claim that the proposed automatic salient object detection algorithm is not only confined to panoramic images but also conventional images and the images with small target.

Conclusion

In this paper, we proposed a novel automatic saliency detection algorithm for panoramic images. We first employed a spatial density pattern detection method using region growing for the panoramic image to obtain the proposal objects. Meanwhile, the fixation prediction model was embedded into the framework to predict the visual attention. Then, the previous saliency information was combined by the maxima normalization to calculate the coarse saliency map. Finally, a geodesic refinement was utilized to get the final saliency map.

Experimental results demonstrated that the proposed saliency detection algorithm provided reliable saliency maps for panoramic images, and outperformed the recent state-of-the-art saliency detection methods qualitatively and quantitatively. Moreover, the proposed algorithm also yielded comparable performance to the existing saliency detection methods on the conventional image dataset with common aspect ratios and small target detection dataset.

Future research topics include the extension of SalPan dataset and the evaluation of saliency detection performance on more diverse panoramic scenes. To encourage future work, we will make the source codes, experiment data, SalPan dataset and other related materials public.

References

- Wang J, Jiang H, Yuan Z, et al. Salient Object Detection: A Discriminative Regional Feature Integration Approach[J]. In *International Journal of Computer Vision*, 2017, 123(2): 251-268.
- Itti L, Koch C, Niebur E. A model of saliency-based visual attention for rapid scene analysis[J]. In *IEEE Transactions on pattern analysis and machine intelligence*, 1998, 20(11): 1254-1259.
- Hou X, Zhang L. Saliency detection: A spectral residual approach[C]. In *Computer Vision and Pattern Recognition, 2007. CVPR'07. IEEE Conference on. IEEE*, 2007: 1-8.
- Alexe B, Deselaers T, Ferrari V. Measuring the objectness of image windows[J]. In *IEEE transactions on pattern analysis and machine intelligence*, 2012, 34(11): 2189-2202.
- Zhu C, Li G, Guo X, et al. A Multilayer Backpropagation Saliency Detection Algorithm Based on Depth Mining[C]. In *International Conference on Computer Analysis of Images and Patterns*. Springer, Cham, 2017: 14-23.
- Itti L. Automatic foveation for video compression using a neurobiological model of visual attention[J]. In *IEEE Transactions on Image Processing*, 2004, 13(10): 1304-1318.

- Salah A A, Alpaydin E, Akarun L. A selective attention-based method for visual pattern recognition with application to handwritten digit recognition and face recognition[J]. In *IEEE transactions on pattern analysis and machine intelligence*, 2002, 24(3): 420-425.
- Frintrop S. General object tracking with a component-based target descriptor[C]. In *Robotics and Automation (ICRA), 2010 IEEE International Conference on. IEEE*, 2010: 4531-4536.
- Rosenholtz R, Dorai A, Freeman R. Do predictions of visual perception aid design?[J]. In *ACM Transactions on Applied Perception (TAP)*, 2011, 8(2): 12.
- Achanta R, Hemami S, Estrada F, et al. Frequency-tuned salient region detection[C]. In *Computer vision and pattern recognition, 2009. cvpr 2009. ieee conference on. IEEE*, 2009: 1597-1604.
- Qin Y, Lu H, Xu Y, et al. Saliency detection via cellular automata[C]. In *Proceedings of the IEEE Conference on Computer Vision and Pattern Recognition*. 2015: 110-119.
- Wei Y, Wen F, Zhu W, et al. Geodesic saliency using background priors[J]. In *Computer Vision - ECCV 2012*, 2012: 29-42.
- Zhu W, Liang S, Wei Y, et al. Saliency optimization from robust background detection[C]. In *Proceedings of the IEEE conference on computer vision and pattern recognition*. 2014: 2814-2821.
- Cheng M M, Warrell J, Lin W Y, et al. Efficient salient region detection with soft image abstraction[C]. In *Proceedings of the IEEE International Conference on Computer vision*. 2013: 1529-1536.
- Margolin R, Tal A, Zelnik-Manor L. What makes a patch distinct[C]. In *Proceedings of the IEEE Conference on Computer Vision and Pattern Recognition*. 2013: 1139-1146.
- Lin C C, Pankanti S U, Natesan Ramamurthy K, et al. Adaptive as-natural-as-possible image stitching[C]. In *Proceedings of the IEEE Conference on Computer Vision and Pattern Recognition*. 2015: 1155-1163.
- Oliva A, Torralba A, Castelhan M S, et al. Top-down control of visual attention in object detection[C]. In *Image processing, 2003. icip 2003. proceedings. 2003 international conference on. IEEE*, 2003, 1: 1-253.
- Gao D, Vasconcelos N. Discriminant saliency for visual recognition from cluttered scenes[C]. In *Advances in neural information processing systems*. 2005: 481-488.
- Gao D, Han S, Vasconcelos N. Discriminant saliency, the detection of suspicious coincidences, and applications to visual recognition[J]. In *IEEE Transactions on Pattern Analysis and Machine Intelligence*, 2009, 31(6): 989-1005.
- Yang J, Yang M H. Top-down visual saliency via joint CRF and dictionary learning[C]. In *Computer Vision and Pattern Recognition (CVPR), 2012 IEEE Conference on. IEEE*, 2012: 2296-2303.
- Shi J, Yan Q, Xu L, et al. Hierarchical image saliency detection on extended CSSD[J]. In *IEEE transactions on pattern analysis and machine intelligence*, 2016, 38(4): 717-729.
- Li H, Lu H, Lin Z, et al. Inner and inter label propagation: salient object detection in the wild[J]. In *IEEE Transactions on Image Processing*, 2015, 24(10): 3176-3186.
- Hou X, Zhang L. Dynamic visual attention: Searching for coding length increments[C]. In *Advances in neural information processing systems*. 2009: 681-688.
- Perazzi F, et al. Saliency filters: Contrast based filtering for salient region detection[C]. In *Computer Vision and Pattern Recognition (CVPR), 2012 IEEE Conference on. IEEE*, 2012: 733-740.
- Kim J S, Sim J Y, Kim C S. Multiscale saliency detection using random walk with restart[J]. In *IEEE transactions on circuits and systems for video technology*, 2014, 24(2): 198-210.
- Luo Y, Yuan J, Xue P, et al. Saliency density maximization for efficient visual objects discovery[J]. In *IEEE Transactions on Circuits and Systems for Video Technology*, 2011, 21(12): 1822-1834.
- Yang C, Zhang L, Lu H. Graph-regularized saliency detection with convex-hull-based center prior[J]. In *IEEE Signal Processing Letters*, 2013, 20(7): 637-640.
- Harel J, Koch C, Perona P. Graph-based visual saliency[C]. In *Advances in neural information processing systems*. 2007: 545-552.
- Cerf M, Harel J, Einhorn W, et al. Predicting human gaze using low-level saliency combined with face detection[C]. In *Advances in neural information processing systems*. 2008: 241-248.
- Borji A. Boosting bottom-up and top-down visual features for saliency estimation[C]. In *Computer Vision and Pattern Recognition (CVPR), 2012 IEEE Conference on. IEEE*, 2012: 438-445.
- Judd T, Ehinger K, Durand F, et al. Learning to predict where humans look[C]. In *Computer Vision, 2009 IEEE 12th international conference on. IEEE*, 2009: 2106-2113.
- Tenenbaum J B, De Silva V, Langford J C. A global geometric framework for nonlinear dimensionality reduction[J]. In *science*, 2000, 290(5500): 2319-2323.
- Zhu W, Liang S, Wei Y, et al. Saliency optimization from robust background detection[C]. In *Proceedings of the IEEE conference on computer vision and pattern recognition*. 2014: 2814-2821.
- Fu K, Gong C, Gu I Y H, et al. Geodesic saliency propagation for image salient region detection[C]. In *Image Processing (ICIP), 2013 20th IEEE International Conference on. IEEE*, 2013: 3278-3282.
- Zhu C, Li G, et al. An Innovative Salient Object Detection Using Center-Dark Channel Prior[C]. In *IEEE International Conference on Computer Vision Workshop (ICCVW) 2017*.
- Lou J, Zhu W, Wang H, et al. Small target detection combining regional stability and saliency in a color image[J]. In *Multimedia Tools and Applications*, 2016: 1-18.